MODERN MEDICINE AND PRACTICE
https://inovatus.es/index.php/ejmmp

EUROPEAN JOURNAL OF MODERNMEDICINEAND PRACTICE
Vol. 4 No. 4 (Apr - 2024) EJMMP ISSN: 2795-921X

SYNTHESIS OF Co_3O_4 NANOPARTICLES AS A PHOTO ANODE FOR NEW DYE SENSITZED SOLAR CELL

Ahmed Radhi Laftah[1*], Mohammed Ahmed Jassima[2], Kawther. H. Jasim[3], Sammah Naeem Ghazi[4]

[1]Ministry of Education General Directorate for Education in the province of Maysan, Iraq

[2]Department of Chemistry, College of Science, Mustansiriyah University, Baghdad, Iraq

[3]Chemistry Department, College of Science, Misan University, Misan, Iraq

[4]Pharmacy Department, Al-Manara College for Medical Sciences, Maysan 62001, Iraq

Abstract: Photovoltaic technology, which makes use of a renewable resource, is one way to address the increasing need for energy on a worldwide scale. Synthesis In this paper, a new azo dye is synthesized and studied using spectroscopy, 1HNMR, UV/visible, Fourier transform infrared spectroscopy, and mass spectroscopy, among other techniques. Solar cells were sensitized using an azo dye. Utilizing transmission electron microscopy, scanning electron microscopy, and X-ray diffraction, the cobalt oxide nanoparticles synthesized by green synthesis were investigated. The size range of nanoparticles is 20-27 nm. A modified Hummer process was used to generate graphene oxide as a cathode, and monolayer and sandwich casting were used to cover the cobalt oxide. Different results were obtained by both methods: Jsc and VO range from 0.531 to 0.5899 V, and conversion efficiencies for the sandwich and single layer techniques are 0.9506% and 1.9373%, respectively. The constructed solar cells outperformed its counterparts in terms of photovoltaic efficiency, which ranged from 2.8557 to 5.5112 (mA/Cm2) percent.

Key words: Cobalt Oxide, Nanoparticles, Solar Cells, FT-IR, Green Synthesis.

1. INTRODUCTION

In the modern world, an energy crisis is a serious problem. When nonrenewable fuels are burned, they significantly increase atmospheric CO2 pollution. Sunlight reaching Earth's surface at an average rate of one watt per hour is more than enough to power the whole planet for an entire year, making renewable energy sources like solar power an attractive choice. [ ]Converting solar energy into a usable form is the holy grail of solar energy research. Solar cells convert sunlight into usable energy by use of a photovoltaic device. popular way for turning solar power into electricity. Free and generated by the sun, solar power is sure to be in a game-changer among future energy alternatives. A dye is used by dye-sensitized solar cells, or DSSCs, to absorb light. Azolo dye's capacity to absorb solar photons is one of many intriguing possibilities for boosting energy sources, decreasing emissions from fossil fuels, and fighting climate change.[ ] The four primary components of a typical DSSC device are the photoanode, photosensitizer, electrolyte, and counter electrode, often known as the cathode. A photo-excited electron is injected at the interface between the semi-conductor material and the monolayer sensitizer, converting visible light energy into electrical energy. This is achieved by making a wide bandgap semi-conductor, such as TiO2, ZnO, or

SnO2, sensitive. the dashA synthetic or natural color is used as the "sensitizer" in DSSCs. Electrons and holes are created by light-sensitive dyeElectrons travel to the semiconductor metal oxide's conduction band, conversely holes go to the electrolyte. Ruthenium compound and other stronger dyes have been created by scientists.[ ] For DSSC to function properly, dye is a necessary component. Dye ideal candidates possess high visible light absorption properties, a semiconductor-attachable moiety, and electron-conducting capabilities.[ ]Broadband sensor semiconductor gaps used to be filled by DSSC using a ruthenium (II) polypyridinic compound, which was costly, complicated, and environmentally harmful. A novel approach employs biodegradable and non-toxic natural pigments derived from plants, fruits, and leaves. The pigments in the pigments absorb the light and convert it into electricity. Both natural and synthetic dyes are safe, inexpensive options.The colors. It must be the ideal initiator.

The following criteria must be satisfied: A sufficiently high LUMO energy level is the first condition. The optimal energy for electron injection at the photoanode's electrode

i) It absorbs solar radiation strongly, with an absorption band that extends from the visible to almost infrared; ii) The space between the dye's positive charge density and Electron injection is large enough to prevent dye degradation; and iii) It has a low HOMO energy level, the oxidized state can regenerate effectively.[ ] A DSSC's photoanode functions as a workstation, absorbing the majority of visible light and moving the charge carriers to a TCO layer. To improve DSSC performance, many methods to change electrode characteristics have been suggested. Among these methods are the production of new nanostructures, the addition of elemental ions by doping, and the development of nanocomposites.[ ] There is a correlation between the complexity and expense of the CE that is responsible for the redox pair regeneration process and the efficiency and cost of the DSSC.[ ] To make cobalt oxide nanoparticles, we applied green chemistry in this study. A new azo dye was created to substitute the more expensive ruthenium dyes used in sensors. The cathode in this setup was an electrode made of graphene oxide nanoparticles. Two distinct methods of electrode deposition were evaluated for their efficacy.

2.Methodology

2.1 Materials

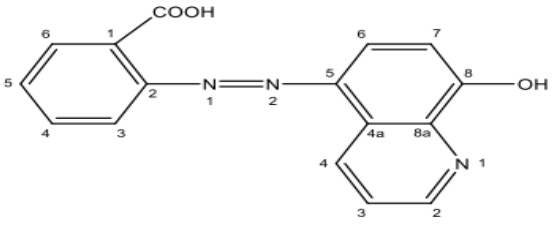
All of the chemicals were given by the Sigma-Aldrich Company and were thereafter used without consideration for their purity. The beetroots, on the other hand, came straight from a local market.

The fresh beetroots were washed extensively with double-distilled water after being purchased from the local farmer's market. After removing the outer layer, the roots were chopped into small pieces and mashed to get a juice with a consistent consistency. iron(II) ionAnthralic acid (C7H7No2), sodium carbonate (Na2CO3), hydrochloric acid (HCl), and sodium nitrite (NaNo2) are the components of the specified mixture. Indium tin oxide (FTO) and ethylene glycol were provided. nonionic water, potassium iodide (KI), iodine (I2), and ethanol (C2H6O) sourced from Sigma-Aldrich, Germany In every experiment, graphene oxide and silver were used as cathodes.

2.2 Preparation of dye as sensitizer

In a 10-milliliter water solution containing 1.3 grams of anthralic acid, 0.5 grams of sodium carbonate were added while stirring the mixture.Temperature of water bath was set to 0–5, and for two minutes, 2.4 cc of strong hydrochloric acid (12 M) was added. To make diazonium salt, add 20% sodium nitrite drop by drop into the solution, then give it a half-hour to rest. Second solution may be made using a 40% sodium hydroxide solution that has been chilled to dissolve 1.2 g of 8-hydroxyquinoline. The diazonium salt is

slowly added to the solution, one drop at a time. For thirty minutes, we saw red downpour. After filtration, the precipitate is cleaned by recrystallization.[ ]

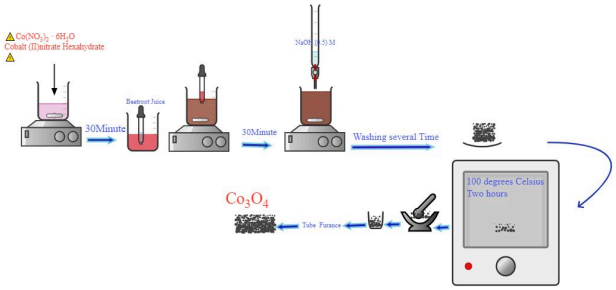


2-((8-hydroxyquinolin-5-yl)diazenyl)benzoic acid
Chemical Formula: $C_{16}H_{11}N_3O_3$

Fig" 2. Strucure of Azo Dye L1

2.3 Preparation Of CO_3O_4 NPs

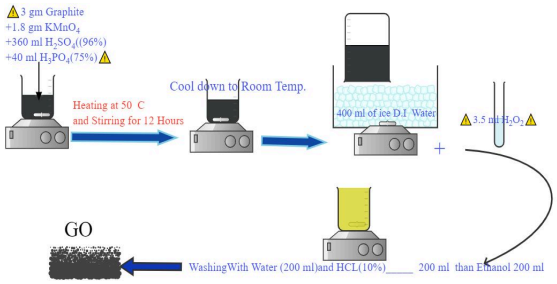
For one hour at 60 degrees Celsius, a stirrer was used to mix 0.01 mol of cobalt nitrate with 50 ml of distilled water. Following this, the pink cobalt nitrate solution was supplemented with 1:2 dark red beetroot juice. It remained agitated for an additional hour after that. The solution's color was changed when a little amount of 0.5 M sodium hydroxide was added, resulting in the precipitation of cobalt particles as a dark pink substance. The solution sedimented to the bottom before disposal. An oven temperature of 120 degrees Celsius was used to dry the solution. for one hour after being rinsed many times with deionized water. Once the hazardous material has been collected. Calcinating the precipitate at 450 degrees followed crushing. Calcination caused the precipitation of dark cobalt oxide.[2]



Fig"3 Scheme preparation of Cobalt Oxide NPs

2.4 Synthesis of Graphene Oxide

A blend of H_2SO_4 and H_3PO_4 was prepared with a volume ratio of 9:1 (180:20 ml). The solution was stirred for 15 minutes before the addition of 1.5 g of powder graphite. Subsequently, 9.0 g of $KMnO_4$ was gently incorporated while swirling the mixture continuously. The blend was stirred consistently for 12 hours. To terminate the process after 12 hours, 4ml of 30% hydrogen peroxide (H2O2) was introduced with 200 ml of chilled deionized water. The mixture was then divided into multiple centrifuge tubes for purification. Purification was achieved by alternating the use of hydrochloric acid (HCl) and deionized (DI) water with centrifugation at 5000 rpm for 15 minutes during each washing stage. This procedure was repeated twice. Finally, the finished product was dried in an oven at 80°C for 24 hours[1].



Fig" 4 Scheme Syntheses of Griffin Oxide NPs

2.5 Solar cell fabrication

FTO (fluorine-doped tin oxide) with multiple coats of glaze (83% transparency, 20 ohm resistance)

Cleansed dried with a hair dryer to remove any last bits of residue after being submerged in an ultrasonic bath of acetone, distilled water and ethanol. A solar-sensitive stain was applied as the next step.

An ethyl acetate and nanopowder oxide mixture was used to create a colloidal solution of cobalt oxide nanostructures for this cell (2,5 * 2 * 0.1 cm). To obtain the optical image, a dropper was used.

For 30 minutes at 200 degrees Celsius, cover the glass's conducting surface with the colloidal solution.

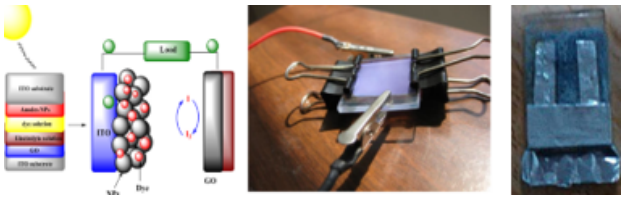
Floating in midair. After the nano-oxides electrode cooled down and was Spin Coated again, it was submerged in an azo dye for 10 hours at room temperature. Graphene oxide was used as the counter electrode. the (I^-/I^-_3) solution, a liquid electrolyte The workspace was penetrated by fall by capillary action, and the binder clip kept the cell in place.[2] It is possible to make an approximation of the fill factor (FF) and the photo-current-voltage (I-V) curve using the equation:

$$ff = \frac{V_{max} * J_{max}}{V_{oc} * J_{sc}} \quad \ldots.(1)$$

Here, Jsc and Voc indicate the photocurrent and photovoltaic at short and open circuits, whereas Imax and Vmax represent the photocurrent and photovoltaic at maximum power output (Pmax), respectively. A DSSC's global solar conversion efficiency (η) is defined as:[3]

$$\eta = \frac{V_{oc} * J_{sc} * ff}{P_{in}} * 100\% \ldots\ldots\ldots(2)$$

power input, denoted by Pin.



Fig". 5 schematic of a functioning DSSC and DSSC construction Double Layer &single Layer

3- Results and discussion

3-1- Infrared spectroscopy through Fourier transforms*Azo Dye*

Figures 4 displays results of FTIR measurements taken in the region of 4000-400 cm1 that were used to calculate the L1. Here is a list, in no particular sequence, of the typical spectral features of phenolic compounds: OH stretching is responsible for the creation of broad band at 3363 and 3223 cm-1, whereas vibrations in plane of bending are responsible for the 1357 cm-1 area. The aromatic C-H bond is accountable for the band seen at 3045 cm-1. Band between 1400 and 1600 cm-1, which may be seen as 1449, 1490, and 1639 cm-1, is thought to be produced by C= C vibrations that stretch occurring inside the aromatic ring as well. The occurrence of many overlapping peaks in the 1200–1300 cm-1 range is indicative of stretching vibrations C–O/C–C. [4]. The band at 1585 cm-1 in the free ligand (L1) corresponds to the (C=N) pyramid group. In most cases, Band about 1490 cm-1 will correspond to the N=N stretching vibration. [5]

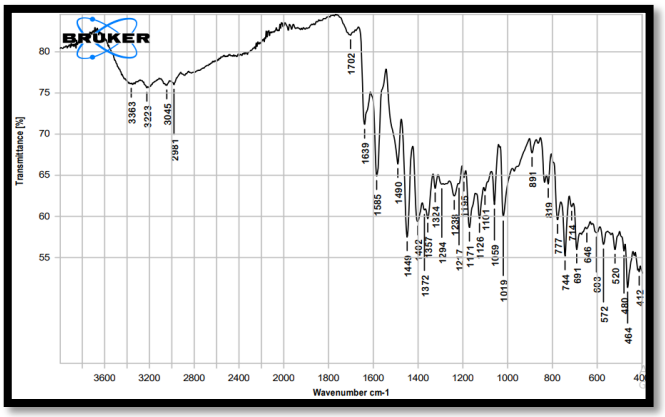


Fig.6 FTIR spectra for the ligand (Azo Dye

3.2 ultraviolet-visible spectroscopy studies

The ultraviolet-visible spectra of ligands showed various band patterns. Bands proposed several distinct groups, which helped design azo dye ligands. 10 $^{-3}$M Room temperature was used to create UV-visible absolute ethanol solutions, and their spectra were noted and evaluated from 200 to 1100 nm. Fig.7. Free ligand (L1) electronic spectra showed two absorption bands. The charge transfer between the azo group (N=N) and the pyramid group (C=N) occurs during the L→L C.T n → n* intermolecular transition was linked to the first band at 485 nm. At 342 nm, there was the (n → π*) band. For the (π-π*) transition, the third band at 281-239 nm was created by the phenyl ring's -systems..[4]

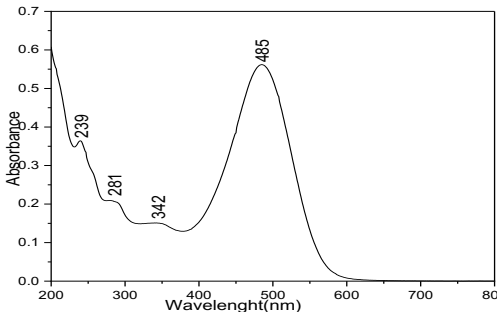


Fig. 7 electronic spectra of ligand Azo Dye

3.3 Mass spectral analysis

A mass spectrometer may help find the ligand's molecular structure. There were numerous peaks visible in the fragmentation ligand's mass spectrum (L1)(fig.8). A low-lying peak at m/z+=293 may be seen in The new Azo ligand's mass spectrum.

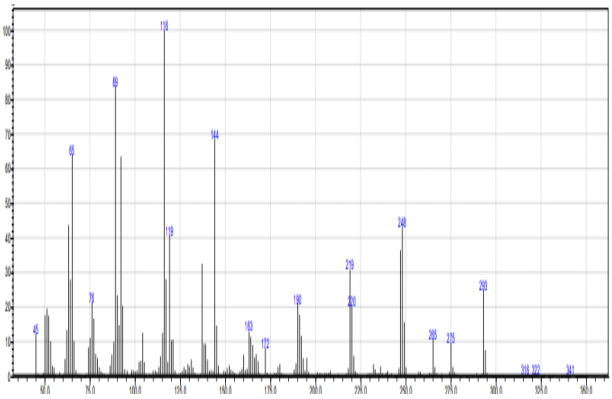


Fig. 8. Azo ligand mass spectrum (L1).

3.4 ^{1}H NMR spectra

Figures 9 prove your point. Using DMSO d6 as the solvent, the ligand's 1H NMR data was examined in ambient temperature with a 400 MHz Bruker spectrometer. The free ligand's low field (L1) the proton of the hydroxyl group (OH) may be the source of the singlet signal seen at (9.54) ppm. Doublets of doublets, or aromatic protons (phenyl rings), were produced by different H-H couplings, and multiples in the (8.19-8.55) ppm range, whereas multiple signals were recorded around 7.35-8.5 ppm due to (M, 9H). The (L1) ligand also displayed an HDO-related singlet signal at (3.67) ppm at the same time. For the solvent proton, there were many well discernible signals at 2.50, 2.51.2.52 ppm.

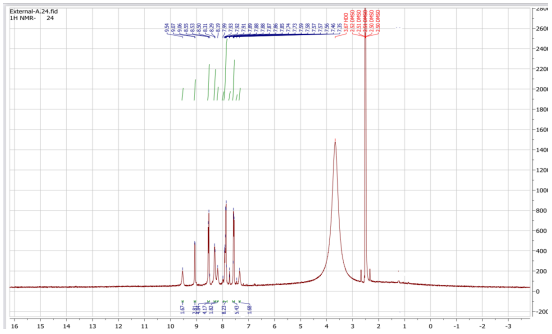


Fig.9. HNMR Spectrum of azo dye ligand

3-5 X-Ray diffraction Co3O4 NPs

The seven hkl planes of CoCo2O4 are (22 0), (311), (222), (4 0 0), (551) and (44 0), according to the data in Figure 8. The JCPDS data card number (80-1538) is widespreadis well-aligned with these hkl planes at 2θ = 59.30, 65.18, 36.77, 44.77, and 31.20 degrees, respectively. The XRD investigation confirmed the absence of contaminants on the peaks, and the results show that the peaks are crisp and intense. The XRD pattern of CoCo2O4f is unique in that it shows peaks for cobalt oxide.[6]

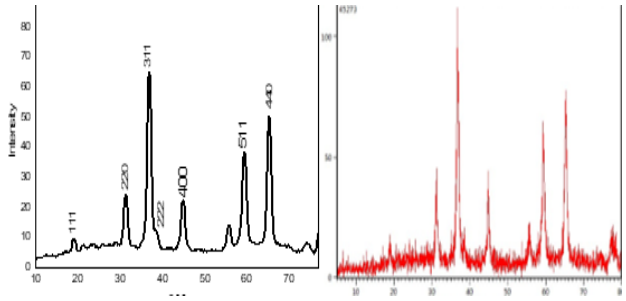


fig. 10 XRD pattern of cobalt oxide nanoparticles

3-6 X-RAY DIFFRACTION OF GRAPHENE OXIDE NPS

Figure 9 . demonstrates the GO's X-ray diffraction (XRD) spectrum. The diffraction peaks happened at 13°, which is the only peak in GO. The (001) crystal plane's reflection was the peak of GO at 2 θ = 13°. Another peak was observed at 2 θ = 43°, which is a portion of the crystal plane (100)[5]

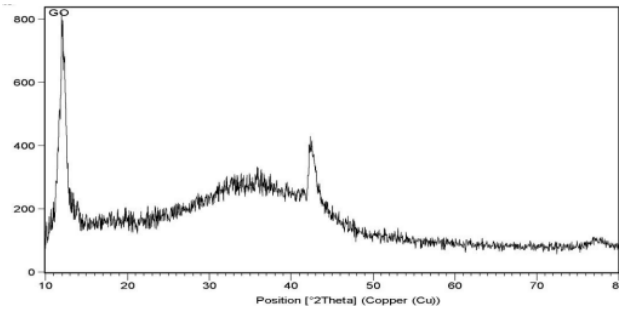


Fig. 11 XRD of G-O nanoparticle

3-7 (FE-SEM) of Co_3O_4 NPs

Fig. 10 shows scanning electron micrographs of the produced green Co3O4 NPs. Particles that have clumped together and are around 23–47 nm in size seem almost spherical in the scanning electron micrograph.

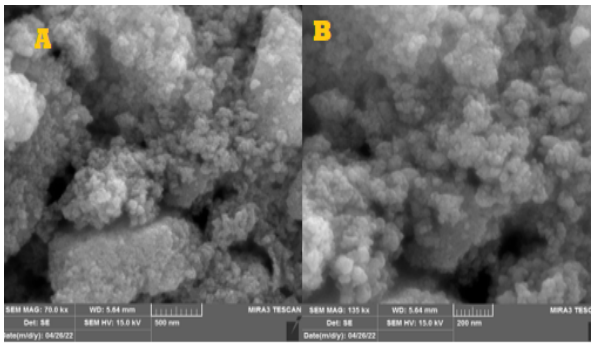


Fig.12. FE-SEM images of Co_3O_4. (a) OverviewFE- SEM image in a low magnification; (b) Enlarged FE-SEM image

3-8 Microscopic studies (TEM) of Co_3O_4

The TEM analysis revealed the shape and size of the cobalt oxide nanoparticles. According to TEM analysis, the average size of Co3O4 NPs was 20 nm, whereas the average size of Ti NPs was 60 nm. Images captured by transmission electron microscopy revealed that the NPS were round and devoid of any cracks or other defects

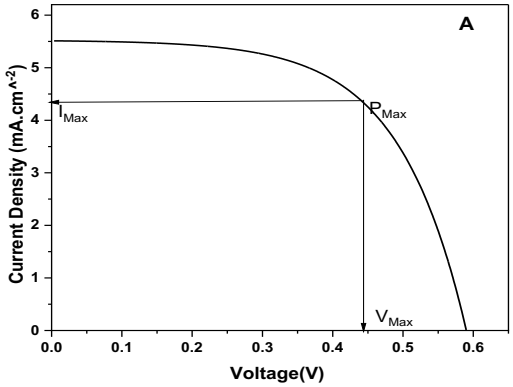
3-9 The Dye-sensitized solar cells parameters

A plot of current vs voltage is constructed to quantify the dye-sensitized solar cell's efficiency. J-V curve are used to analyze maximum power of a built DSSC, and The efficiency () and fill factor (FF) are determined under illumination. Equated using an irradiation of about 100 mW/cm2.

$$ff = \frac{V_{max} * J_{max}}{V_{oc} * J_{sc}} \ldots\ldots\ldots\ldots (1)$$

$$\eta = \frac{V_{oc} * J_{sc} * ff}{P_{in}} * 100\% \ldots\ldots\ldots\ldots (2)$$

Your total is.100. The Efficiency of Power Conversion of the newly built DSSC was evaluated using an analyzer. The J-V curve and a Peccell Solar Simulator with a 100 W power output were used for this evaluation. The J-V curve intercepts establish the operational characteristics. These characteristics include the fill factor (FF), open-circuit voltage (Voc), conversion efficiency (%), and short-circuiting current density (Jsc). Using the J-V characteristic data, we were able to estimate the output power of the constructed DSSC.the dash you can see all the solar cell data from this study in the table and visuals below.



Figure(14A) J–V plot of Co_3O_4 (one Lyer)

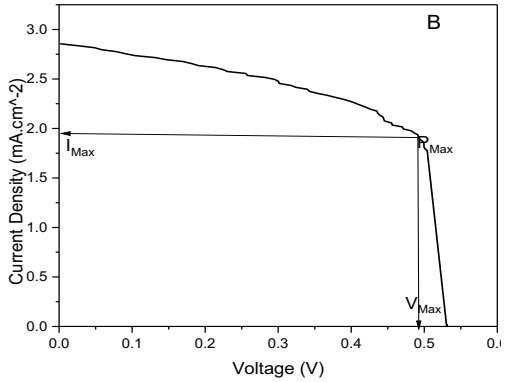


Figure14b J–V plot of Co_3O_4 (Sandwish)

Table 1. Solar cell parameters of dye sensitizer solar cell for (Co_3O_4/nano L1/GO)

method	FF	η %	Voc(V)	Jsc (mA/cm^2)	MP (W/cm^2
Double Layer	62..68	0.950	0.531	2.855	0.950
One Layer	59.59	1.937	0.589	5.511	1.937

With VO ranging from 0.5896 to 0.5899 V and Jsc from 2.7556 to 5.5112 (mA/Cm2), respectively, and an anode of green-made Co3O4 photocatalyst and a cathode of graphene produced the best results (0.9686 and 1.9373% efficiencies, respectively), which may highlight the significance of graphene as a cathode. Additionally, DSSCs performed better when the cell was operating from a single layer.[6]

4- Conclusion

This study developed a new dye by combining organic azo dyes; it was then tested using various techniques. As a sensitizer, it was used by the dye solar cell. It served as an effective safeguard. The cathode electrode was made of graphene oxide, while the photo anode was cobalt oxide. Multiple techniques were used to find the electrode. In comparison to the first method, drop coasting—in which the first and second layers are each one-and-a-half layers—was shown to improve cell efficiency, filling factor, and current less than the first method.

References

1) Abdul-Ameer Aboud, Nibras, Wafaa M.S Alkayat, Dhia H Hussain, Ahmed Mahdi Rheima, 'A comparative study of ZnO, CuO and a binary mixture of ZnO 0.5 -CuO 0.5 with nano-dye on the efficiency of the dye-sensitized solar cell', *Journal of Physics: Conference Series*, vol. 1664, no. 1, November 2020, p. 012094.

2) Adedokun, Oluwaseun, Mojoyinola Kofoworola Awodele, Yekinni Kolawole Sanusi, Ayodeji Oladiran Awodugba, 'Natural dye extracts from fruit peels as sensitizer in ZnO-based dye-sensitized solar cells', *IOP Conference Series: Earth and Environmental Science*, vol. 173, no. 1, 2018.

3) Aghazada, Sadig, Mohammad Khaja Nazeeruddin, 'Ruthenium complexes as sensitizers in dye-sensitized solar cells', *Inorganics*, vol. 6, no. 2, June 2018.

4) Al-Adilee, Khalid J; Dakheel, Haitham K, 'Synthesis, spectral and biological studies of Ni (II), Pd (II), and Pt (IV) complexes with new heterocyclic ligand derived from azo-Schiff bases dye', *Eurasian Journal of Analytical Chemistry*, vol. 18, no. 5, 2018.

5) Alshamsi, Hassan A.Habeeb, Khalid J. AL-Adilee, Suadad A. Jaber, 'Thermal decomposition study on solid complexes of 7-[2-(benzimidazolyl)azo]-8-hydroxy quinoline with Co(III), Ni(II) and Cu(II)', *Oriental Journal of Chemistry*, vol. 31, no. 2, 2015, pp. 809–817.

6) Al Batty, Sirhan, Sama M. Al-Jubouri, Mohammed Wali Hakami, Abdulla Sarief, SK Manirul Haque, 'Innovative economic anthocyanin dye source for enhancing the performance of dye-sensitized solar

cell', *Journal of Taibah University for Science*, vol. 16, no. 1, 2022, pp. 415–422.

7) Chindeka, Francis, Philani Mashazi, Jonathan Britton, David O. Oluwole, Sivuyisiwe Mapukata, Tebello Nyokong, 'Fabrication of dye-sensitized solar cells based on push-pull asymmetrical substituted zinc and copper phthalocyanines and reduced graphene oxide nanosheets', *Journal of Photochemistry and Photobiology A: Chemistry*, vol. 399, August 2020, p. 112612.

8) Coates, John, 'Interpretation of Infrared Spectra, A Practical Approach', *Encyclopedia of Analytical Chemistry*, 2006, pp. 1–23.

9) Cuce, Erdem, Saffa B. Riffat, Chin Huai Young, 'Thermal insulation, power generation, lighting and energy saving performance of heat insulation solar glass as a curtain wall application in Taiwan: A comparative experimental study', *Energy Conversion and Management*, vol. 96, 2015, pp. 31–38.

10) David, Samuel Alwin, Asirvatham Doss, Rajamma Powel Praveen Pole, Thankappan Pushpabai Kumari Pushpa Rani, Raveendran Padma Latha Reshmi, Ramakrishnan Rajalakshmi, 'Synthesis and characterization of Cobalt Oxide nanoparticles using Momordica charantia and its photocatalytic activity', *International Journal of Nano Dimension*, vol. 13, no. 3, 2022, pp. 335–343.

11) Etesami, Hadi, Mohammad Mansouri, Adnan Habibi, Farhad Jahantigh, 'S7ynthesis and investigation of double alternating azo group in novel para-azo dyes containing nitro anchoring group for solar cell application', *Journal of Molecular Structure*, vol. 1203, March 2020, p. 127432.

12) Hidayah, N. M. S., Wei-Wen Liu, Chin-Wei Lai, N. Z. Noriman, Cheng-Seong Khe, U. Hashim, H. Cheun Lee, 'Comparison on graphite, graphene oxide and reduced graphene oxide: Synthesis and characterization', 150002, 2017.

13) Jadhav, C. H., K. B. Pisal, A. R. Chavan, S. M. Patil, P. B. Patil, P. K. Pagare, 'Electrochemical supercapacitive performance study of spray pyrolyzed cobalt oxide film', *Materials Today: Proceedings*, vol. 43, no. xxxx, 2020, pp. 2742–2746.

14) Kaya, Ismail Cihan, Seckin Akin, Hasan Akyildiz, Savas Sonmezoglu, 'Highly efficient tandem photoelectrochemical solar cells using coumarin6 dye-sensitized CuCrO2 delafossite oxide as photocathode', *Solar Energy*, vol. 169, July 2018, pp. 196–205.

15) Kumar, Pushpendra, Santhosh Penta, Shyama Prasad Mahapatra, 'Synthesis and Dielectric Relaxation Spectroscopy of Graphene Oxide Nanoparticles: Effects of Frequency, Thickness, and Temperature', *Journal of Electronic Materials*, vol. 49, no. 10, 2020, pp. 5801–5807.

16) Liu, Jun, Jian feng Lu, Juan Kan, Xiao yuan Wen, Chang hai Jin, 'Synthesis, characterization and in vitro anti-diabetic activity of catechin grafted inulin', *International Journal of Biological Macromolecules*, vol. 64, 2014, pp. 76–83.

17) Mahmoud, Zaid H., Reem Adham AL-Bayati, Anees A. Khadom, 'Electron transport in dye-sanitized solar cell with tin-doped titanium dioxide as photoanode materials', *Journal of Materials Science: Materials in Electronics*, vol. 33, no. 8, 2022, pp. 5009–5023.

18) Mezgebe, Kibrom, Endale Mulugeta, 'Synthesis and pharmacological activities of azo dye derivatives incorporating heterocyclic scaffolds: a review', *RSC Advances*, vol. 12, no. 40, 2022, pp. 25932–25946.

19) Najm, Asmaa Soheil, Norasikin A. Ludin, Mahir Faris Abdullah, Munirah A. Almessiere, Naser M. Ahmed, Mahmoud A.M. Al-Alwani, 'Areca catechu extracted natural new sensitizer for dye-sensitized

solar cell: performance evaluation', *Journal of Materials Science: Materials in Electronics*, vol. 31, no. 4, February 2020, pp. 3564–3575.

20) Narayan, Monishka Rita, 'Review : Dye sensitized solar cells based on natural photosensitizers', *Renewable and Sustainable Energy Reviews*, vol. 16, no. 1, 2012, pp. 208–215.

21) Ozturk, T., B. Gulveren, M. Gulen, E. Akman, S. Sonmezoglu, 'An insight into titania nanopowders modifying with manganese ions: A promising route for highly efficient and stable photoelectrochemical solar cells', *Solar Energy*, vol. 157, 2017, pp. 47–57.

22) P.Solomon, K . Nakanish and, 'Infrared Absorption Spectroscopy', *HOLDEN DAY*, 1977.

23) Polo, André Sarto, Neyde Yukie Murakami Iha, 'Blue sensitizers for solar cells: Natural dyes from Calafate and Jaboticaba', *Solar Energy Materials and Solar Cells*, vol. 90, no. 13, 2006, pp. 1936–1944.

24) Prakash, Pooja, B. Janarthanan, Mohd Ubaidullah, Abdullah M. Al-Enizi, Shoyebmohamad F. Shaikh, Nouf B. Alanzi, Rayana Ibrahim Alkhalifah, Mohammad Ilyas, 'Optimization, Fabrication, and Characterization of Anthocyanin and Carotenoid derivatives based Dye-Sensitized Solar Cells', *Journal of King Saud University - Science*, March 2023, p. 102625.

25) Robertson, Neil, 'Optimizing dyes for dye-sensitized solar cells', *Angewandte Chemie - International Edition*, vol. 45, no. 15, 2006, pp. 2338–2345.

26) Sinha, Keka, Papita Das Saha, Siddhartha Datta, 'Extraction of natural dye from petals of Flame of forest (Butea monosperma) flower: Process optimization using response surface methodology (RSM)', *Dyes and Pigments*, vol. 94, no. 2, 2012, pp. 212–216.